Synthesis and Characterization of Mn-Containing Cubic Mesoporous MCM-48 and AlMCM-48 Molecular Sieves

Jie Xu,[†] Zhaohua Luan,[†] Martin Hartmann,[‡] and Larry Kevan*,[†]

Department of Chemistry, University of Houston, Houston, Texas 77204-5641, and Department of Chemistry, Chemistry Technology, University of Kaiserslautern, P.O. Box 3049, D-67653 Kaiserslautern, Germany

Received May 18, 1999. Revised Manuscript Received July 29, 1999

Employing electron spin resonance (ESR) and electron spin echo modulation (ESEM) spectroscopy, five Mn(II) species are found in three kinds of Mn-containing MCM-48 materials: ion-exchanged Mn−MCM-48, synthesized MnMCM-48, and synthesized MnMCM-48(Ca) with subsequent $CaCl_2$ exchange. Mn(II) species I with a well-resolved sextet centered at $g = 2.00$ has distorted octahedral symmetry and is observed in hydrated ion-exchanged Mn−MCM-48 and in synthesized calcined MnMCM-48. Mn(II) species II with a group of single peaks between $g = 11.32$ and 2.62 with possible distorted tetrahedral symmetry and a significant zero field contribution is observed in dehydrated Mn−MCM-48 and in MnMCM-48. Mn(II) species III with a symmetric line at $g = 2.00$ and a line width around 410 G is assigned to tetrahedral symmetry and is observed in MnMCM-48(Ca) and in MnAlMCM-48(Ca). Mn(II) species IV with a sextet centered from 4.11 to 4.34 also has distorted octahedral symmetry and is obtained in partially dehydrated Mn−MCM-48 and Mn−AlMCM-48. Mn(II) species V with a peak at $g = 5.70$ has distorted tetrahedral symmetry and is produced in dehydrated or hydrogen reduced MnMCM-48. Mn(II) species I, II and IV correspond to extraframework Mn(II), and Mn(II) species III and V are assigned to framework sites. Extraframework Mn(II) species I and II coordinate with four D_2O molecules and are accessible to water, but framework Mn(II) species III coordinates with only three D_2O molecules and is less accessible to water. Similar results are also obtained for Mn-containing AlMCM-48 materials.

Introduction

The discovery of ordered M41S-type mesoporous molecular sieves has been an active research area in recent years.[1,2] This novel family of materials possesses uniform hexagonal (MCM-41) and cubic (MCM-48) pore systems ranging from 10 to more than 100 Å.[3,4] To generate potential catalysts, several transition-metal-modified MCM-41 materials have been synthesized,[5−13] and some are more active than microporous catalysts.[5−8,12] However, transition-metal-modified MCM-48 materials have been less studied, probably due to the difficulty of reliable synthesis.[14−16] For catalytic applications, MCM-48 with its three-dimensional channel system seems to be more advantageous than MCM-41 with one-dimensional channels, because MCM-48 is more resistant to pore blocking and allows faster diffusion.

In this work, manganese-modified MCM-48 materials were synthesized and studied by electron spin resonance (ESR) coupled with electron spin echo modulation (ESEM). ESR spectroscopic data give information about the coordination symmetry of Mn(II) ions. ESEM probes the local environment of Mn(II) species and yields information on the coordination number and interaction distance of adsorbate molecules.[17] Manganese ion is a useful probe because Mn(II) and Mn(IV) ions have ESR spectra that are very sensitive to the local environment.[18−21] Manganese ions in zeolites or oxide materials are also effective for catalyzing ethylene hydrogena-

[†] University of Houston.
[‡] University of Kaiserslautern.

(1) Kresge, C. T.; Leonowicz, M. E.; Roth, W. J.; Vartuli, J. C.; Beck, J. S. *Nature* **1992**, *359*, 710.
(2) Beck, J. S.; Vartuli, J. C.; Roth, W. J.; Leonowicz, M. E.; Kresge, C. T.; Schmitt, K. D.; Chu, C. T.-W.; Olson, D. H.; Sheppard, E. W.; McCullen, S. B.; Higgins, J. B.; Schlenker, J. L. *J. Am. Chem. Soc.* **1992**, *114*, 10834.
(3) Casci, J. L. *Stud. Surf. Sci. Catal.* **1994**, *85*, 329.
(4) Sayari, A. *Chem. Mater.* **1996**, *8*, 1840.
(5) Corma, A. *Chem. Rev.* **1997**, *97*, 2373.
(6) Notari, B. *Catal. Today* **1993**, *18*, 163.
(7) Kresge, C. T.; Leonowicz, M. E.; Roth, W. J.; Vartuli, J. C. U.S. Patent 5,250,282,1993.
(8) Corma, A.; Navarro, M. T.; Porez-Pariente, J. *J. Chem. Soc., Chem. Commun.* **1994**, 147.
(9) Pöppl, A.; Baglioni, P.; Kevan, L. *J. Phys. Chem.* **1995**, *99*, 14156.
(10) Zhao, D. Y.; Goldfarb, D. *J. Chem. Soc., Chem. Commun.* **1995**, 875.
(11) Xu, J.; Luan, Z.; Wasowicz, T.; Kevan, L. *Microporous Mesoporous Mater.* **1998**, *22*, 179.
(12) Reddy, K. M.; Moudrakovski, I.; Sayari, A. *J. Chem. Soc., Chem. Commun.* **1994**, 1059.
(13) Luan, Z.; Xu, J.; He, H. Y.; Klinowski, J.; Kevan, L. *J. Phys. Chem.* **1996**, *100*, 19995.
(14) Zhang, W. Z.; Pinnavaia, T. J. *Catal. Lett.* **1996**, *38*, 261.
(15) Morey, M.; Davidson, A.; Stucky, G. *Microporous Mater.* **1996**, *6*, 99.
(16) Hartmann, M.; Racouchot, S.; Bischof, C. *Microporous Mesoporous Mater.* **1999**, *27*, 309.
(17) Kevan, L. *Acct. Chem. Res.* **1987**, *20*, 1.
(18) De Vos, D. E.; Weckhuysen, B. M.; Bein, T. *J. Am. Chem. Soc.* **1996**, *118*, 9615.
(19) Brouet, G.; Chen, X.; Lee, C. W.; Kevan, L. *J. Am. Chem. Soc.* **1992**, *114*, 3720.

10.1021/cm990300j CCC: $18.00
Published on Web 09/24/1999

tion,[22] oxidative coupling of methane,[23] and oxidation of NO.[24] ESR and ESEM techniques have been successfully applied in our previous work on Mn-containing MCM-41 materials.[11]

Three classes of Mn-containing MCM-48 samples are studied in this work. One is liquid phase Mn(II) ion-exchanged MCM-48, denoted Mn−MCM-48 or Mn−AlMCM-48-(*n*), where *n* is the Si/Al ratio. The second is synthesized material, denoted MnMCM-48 or MnAlMCM-48, where the Mn(II) salt is added to the synthesis gel. The third is $CaCl_2$-exchanged, synthesized MCM-48, in which the residual extraframework Mn(II) ions are ion-exchanged by Ca(II) ions,[19] denoted by MnMCM-48(Ca) or MnAlMCM-48(Ca). ESR and ESEM studies show differences among these samples for dehydration, oxidation, reduction, and rehydration treatments. The results are explained in terms of partial incorporation of Mn(II) into the framework of synthesized MnMCM-48 or MnAlMCM-48 materials.

Experimental Section

Synthesis. Pure silicate MCM-48 materials were synthesized as described previously.[25] Mn-containing MCM-48 samples are obtained by adding manganese acetate, $Mn(OAc)_2$ (Allied Chemical) to the gel during the synthesis.

Tetraethyl orthosilicate from Aldrich Chemical (10 mL) was added to an aqueous solution containing 88 g of 10 wt % cetyltrimethylammonium bromide solution (CTAB, Aldrich Chemical) and 10 mL of 2 M NaOH (EM Industries). After being stirred for several minutes, the mixture becomes cloudy, indicating the onset of some silica precipitation, and then, different amounts of $Mn(OAc)_2$ were added and coprecipitated with the silica. After being stirred for 0.5 h, the homogeneous gel was transferred to a Teflon bottle and crystallized under static hydrothermal conditions at 373 K for 72 h. The molar composition of the final gel mixture was SiO_2 (0−0.005):Mn (0.23):Na_2O (0.55):CTAB (112):H_2O. The product was filtered, thoroughly washed with deionized water, and dried at 353 K overnight. The as-synthesized samples were then calcined at 823 K first in flowing nitrogen for 1 h and then in flowing oxygen for 14 h to remove the CTAB. The color of the manganese-containing samples is light pink. The resulting samples are denoted as MnMCM-48.

Al-containing MCM-48 samples were also synthesized by this procedure. Aluminum is introduced together with the tetraethyl orthosilicate. The molar composition of the final gel mixture was SiO_2 (0−0.005):Mn (0.002−0.0125): Al_2O_3 (0.23−0.43):Na_2O (0.55): CTAB (154): H_2O. These samples are labeled AlMCM-48-(*n*) or MnAlMCM-48-(*n*), where *n* indicates the Si/Al ratio.

Liquid-state Mn(II) ion-exchanged samples were prepared by stirring 1 g of calcined MCM-48 or AlMCM-48 in 100 mL of 0.002 M $Mn(OAc)_2$ solution for 6 h. The material was then filtered and washed at 343 K by deionized water in order to remove any ions adsorbed on the external surface. These ion-exchanged samples are denoted as Mn−MCM-48 or Mn−AlMCM-48.

The $CaCl_2$-exchanged samples were obtained by stirring 1 g of calcined MnMCM-48 or MnAlMCM-48 in 100 mL of a 0.05 M $CaCl_2$ solution at 333 K for 4 h to attempt to exchange Ca(II) for some extraframework Mn(II).[11,19] The resulting samples are denoted MnMCM-48(Ca) or MnAlMCM-48(Ca) to distinguish them from the original synthesized samples. This process was repeated if necessary.

Characterization. Powder X-ray diffraction (XRD) patterns were collected using a Philips 1840 powder diffractometer with Cu Kα radiation (40 kV, 25 mA) at 0.025° step size and 1 s step time over a $1.5° < 2\theta < 15°$ range. The samples were prepared as thin layers on metal slides.

N_2 adsorption isotherms were measured at 77 K using a Micromeritics Gemini 2375 analyzer. The volume of adsorbed N_2 was normalized to standard temperature and pressure. Prior to adsorption, the samples were dehydrated at 573 K for 5 h. The specific surface area, A_{BET}, was determined from the linear part of the BET equation. The pore size distribution was calculated from the desorption branches of the N_2 adsorption isotherm using the Barrett−Joyner−Halenda (BJH) formula.[26−28]

^{27}Al magic-angle-spinning (MAS) NMR spectra were recorded at 104.3 MHz with 0.5 s recycle delays. External Al$(H_2O)_6^{3+}$ was used as a reference. Thermogravimetric analysis (TGA) was carried out in air on a TA Instruments thermal analyzer at a heating rate of 3 K/min. The elemental composition was analyzed by electron probe microanalysis using a JEOL JXA-8600 spectrometer.

For ESR and ESEM measurements, calcined and hydrated samples were loaded into 3 mm o.d. by 2 mm i.d. Suprasil quartz tubes. Completely dehydrated samples are obtained by first evacuating in a vacuum ($P < 10^{-4}$ Torr) at 293 K for 14 h, then gradually heating to 393 K in a vacuum and maintaining at this temperature for another 14 h, and finally, heating at 623 K for 4 h in a vacuum. Oxidized or reduced samples were obtained by heating dehydrated samples under oxygen or hydrogen atmosphere (50−100 Torr) at 623 K for 4−14 h. Adsorption was done by exposing dehydrated samples to D_2O (Aldrich), CH_3OD, or CD_3OH (Stohler Isotope Chemicals) at their room-temperature vapor pressures for 14 h. ND_3 (Stohler Isotope Chemicals) was adsorbed at 100 Torr for 1 day, and C_2D_4 (Cambridge Isotope Laboratories) was adsorbed at 50 Torr for 3−21 days.

X-band (9 GHz) ESR spectra were recorded at 77 K on a Bruker ESP 300 spectrometer. The relative ESR intensities were calculated by double integration of the ESR signals. The ESEM modulation were recorded at 4 K on an ESP 380 Bruker FT ESR spectrometer using a $\pi/2-\tau-\pi/2-T-\pi/2$ pulse sequence as a function of T.[29] Different values of τ in a three-pulse experiment were selected to minimize the ^{27}Al modulation.[29] The time-domain deuterium ESEM modulation was analyzed by a spherical approximation for powder samples in terms of N nuclei at distance R with an isotropic hyperfine coupling A_{iso}, where the modulation function is simulated and fitted to the experimental data by a least-squares procedure.[30]

Results

XRD. An XRD pattern characteristic of the MCM-48 structure[3,4] is observed for as-synthesized and calcined MCM-48, MnMCM-48 (Si/Mn = 200), AlMCM-48-(50) and MnAlMCM-48-(50) (Si/Mn = 500). The eight XRD reflection peaks from 2 to 6° 2θ are all reasonably well resolved and in good agreement with reported patterns from MCM-48 materials.[2,31,32] The peak resolution is worse after a larger amount of aluminum or manganese

(20) Levi, Z.; Raitsimring, A. M.; Goldfarb, D. *J. Phys. Chem.* **1991**, *95*, 5, 7830.
(21) Schreurs, J. W. H. *J. Chem. Phys.* **1978**, *69*, 2151.
(22) Baltanas, M. A.; Stiles, A. B.; Katzer, J. R. *Appl. Catal.* **1986**, *28*, 13.
(23) Wang, D.; Rosynek, M. P.; Lunsford, J. H. *J. Catal.* **1995**, *155*, 390.
(24) Kapteijn, F.; Singoredjo, L.; Driel, M.; Andreini, A.; Moulijn, J. A.; Ramis, G.; Busca, G. *J. Catal.* **1994**, *150*, 105.
(25) Xu, J.; Luan, Z.; He, H.; Zhou, W.; Kevan, L. *Chem. Mater.* **1998**, *10*, 3690.
(26) Tanev, P. T.; Vlaev, L. T. *J. Colloid Interface Sci.* **1993**, *160*, 110.
(27) Naono, H.; Hakuman, M.; Nakal, K.; *J. Colloid Interface Sci.* **1994**, *165*, 532.
(28) Barrrett, E. P.; Joyner, L. G.; Halenda, P. P. *J. Am. Chem. Soc.* **1951**, *73*, 373.
(29) Kevan, L. In *Time Domain Electron Spin Resonance*; Kevan, L., Schwartz, R. N., Eds.; Wiley: New York, 1979; p 279.
(30) Kevan, L.; Bowman, M. K.; Narayana, P. A.; Boeckman, R. K.; Yudanov, V. F.; Tsvetkov, Yu. D. *J. Chem. Phys.* **1975**, *63*, 409.

is added to the synthesis gel. No MCM-48 structure can be produced at Si/Al ratios lower than 30 or Si/Mn ratios lower than 200 under these synthesis conditions. After calcination, the XRD reflections increase in intensity and move to a lower angle. This corresponds to further silicon condensation and contraction of the MCM-48 framework during calcination.

N_2 Adsorption Isotherms. Low-temperature nitrogen adsorption isotherms enable the calculation of the specific surface area and the mesopore size distribution. All calcined samples show a typical reversible type IV adsorption isotherm as defined by IUPAC.[33] The sharp inflection between relative pressure $P/P_0 = 0.2$ and 0.3 in these isotherms corresponds to capillary condensation within uniform mesopores. The sharpness of this step reflects the uniform pore size in these materials.[34] The corresponding BJH plots of the derivative of the pore volume per unit weight with respect to the pore diameter (dV/dD) versus the pore diameter are calculated. A very narrow pore size distribution is observed in these four samples. The BET surface areas were calculated[34] with a 16.2 Å cross-sectional area of nitrogen and are larger than 1500 m^2/g for all samples. Therefore, these four samples possess a very uniform pore structure and high surface area.

^{27}Al MAS NMR. To study the aluminum environment, both as-synthesized and calcined Al-containing MCM-48 materials were measured by ^{27}Al MAS NMR. Only a single peak around 54 ppm relative to $Al(H_2O)_6^{3+}$ is observed in as-synthesized AlMCM-48-(50), calcined AlMCM-48-(50), and calcined MnAlMCM-48-(50) (Si/Mn = 500). This indicates that all of the aluminum is in tetrahedral coordination even after calcination.[11,35]

Thermogravimetric Analysis. The thermogravimetric analysis (TGA) curves of as-synthesized MCM-48 and MnMCM-48 where the Si/Mn ratio is 200 are shown in Figure 1a,b. The initial small weight loss around 373 K is due to the desorption of physically adsorbed water. The removal of organic surfactants is completed in two steps (at 513 and 573 K) in MCM-48 (Figure 1a) and in three steps (at 513, 573, and 727 K) in MnMCM-48 (Figure 1b). This high-temperature weight loss (727 K) is also observed in the TGA measurement of as-synthesized AlMCM-48-(50) (Figure 1c) where the aluminum is tetrahedrally incorporated into framework sites as indicated by ^{27}Al MAS NMR. The low-temperature weight loss around 513 and 573 K in those samples is assigned to the decomposition of CTAB surfactant occluded inside the channels. The high-temperature weight loss at 727 K observed in MnMCM-48 and AlMCM-48-(50) is assigned to the decomposition of protonated amines balancing the framework negative charge resulting from the incorporation of manganese or aluminum into MCM-48.[36]

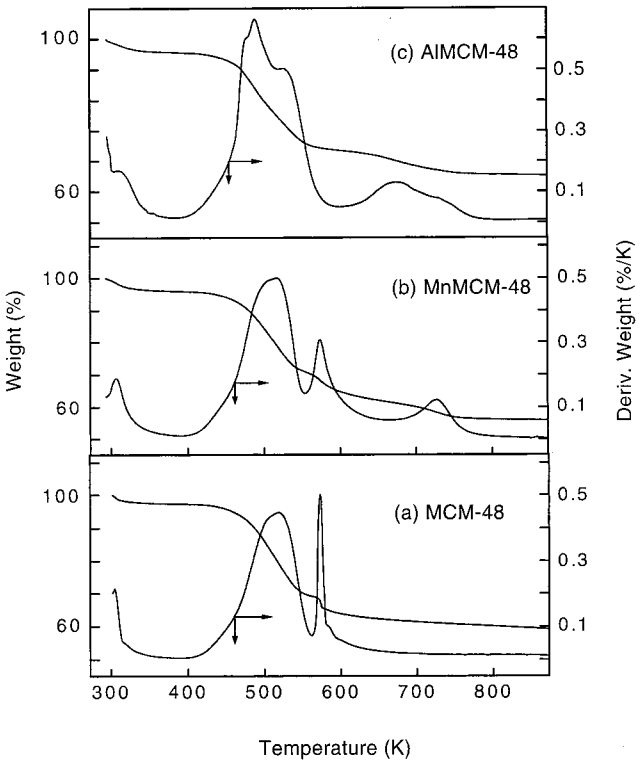

Figure 1. TGA curves of as-synthesized samples: (a) MCM-48, (b) MnMCM-48, and (c) AlMCM-48. The Si/Al ratio is 50 and the Si/Mn ratio is 200 in the synthesis gel.

ESR after Dehydration, Oxygen and Hydrogen Treatments. All three types of Mn-containing MCMM-48 materials, Mn(II) ion-exchanged, synthesized, and $CaCl_2$-exchanged synthesized samples, were studied after dehydration, oxygen oxidation, and hydrogen-reduction treatments. To obtain well-resolved ESR spectra, the manganese concentrations were controlled to a Si/Mn ratio of around 1000 for both synthesized and ion-exchanged Mn-containing samples. In addition, the silicon-to-aluminum ratio was fixed to 50.

The 77 K ESR spectra of Mn(II) ion-exchanged Mn−MCM-48 (Si/Mn ≈ 1000) after dehydration, oxidation, and reduction treatments are shown in Figure 2. The Mn(II) ions are at extraframework sites. In a fresh sample, only a typical sextet from ^{55}Mn ($I = {}^5/_2$) interaction with a g value of 2.00 and an averaged hyperfine parameter A of 97 G is observed (Figure 2a). This signal is also observed in Mn−MCM-41 materials[10,11] and in many zeolites.[18−20] It is an octahedrally symmetric Mn(II) species and is assigned to Mn(II) species I. Under gradual dehydration from 293 to 623 K, many new ESR peaks around g values of 11.32, 5.20, 3 0.20, and 2.62 (Figure 2b,c) appear and are assigned to Mn(II) species II. After heating to 623 K for 4 h, the sample is considered to be dehydrated completely. The original Mn(II) species I now is replaced by a new broad symmetric peak with a peak-to-peak line width of about 410 G (Figure 2c). This new peak is assigned to Mn(II) species III. Subsequent oxidation produces a very broad peak around $g = 2.62$ with peak-to-peak line width of around 832 G (Figure 2d). This broad peak is probably due to oxygen directly coordinated to Mn(II) ions. Hydrogen reduction recovers Mn(II) species III as shown

(31) Vartuli, J. C.; Schmitt, K. D.; Kresge, C. T.; Roth, W. J.; Leonowicz, M. E.; McCullen, S. B.; Hellring, S. D.; Beck, J. S.; Schlenker, J. L.; Olson, D. H.; Sheppard, E. W. *Chem. Mater.* **1994**, *6*, 2317.
(32) Huo, Q.; Margolese, D. I.; Stucky, G. D. *Chem. Mater.* **1996**, *8*, 1147.
(33) Brunauer, S.; Deming, L. S.; Deming, W. S.; Teller, E. *J. Am. Chem. Soc.* **1940**, *62*, 1723.
(34) Sing, K. S. W.; Everett, D. H.; Haul, R. A. W.; Moscou, L.; Pierotti, R. A.; Rouquerol, J.; Siemieniewska, T. *Pure Appl. Chem.* **1985**, *57*, 603.
(35) Hartmann, M.; Bischof, C. *Stud. Surf. Sci. Catal.* **1998**, *117*, 249.
(36) Prakash, A. M.; Wasowicz, T.; Kevan, L. *J. Phys. Chem.* **1996**, *100*, 15947.

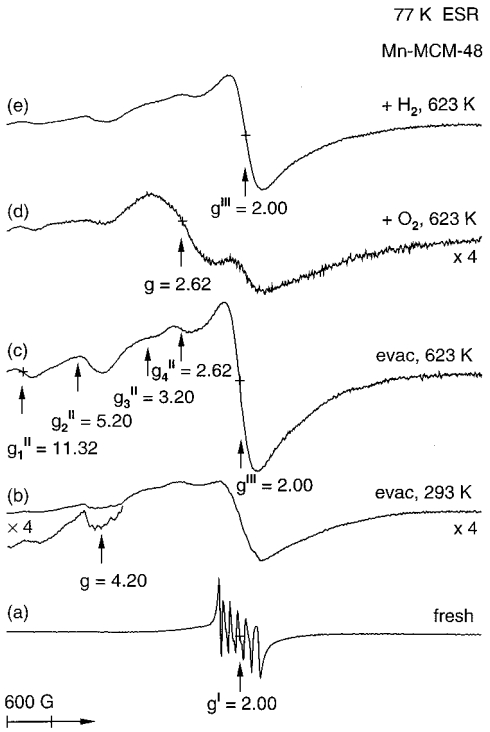

Figure 2. ESR spectra at 77 K of ion-exchanged Mn−MCM-48: (a) fresh, (b) evacuation at 293 K, (c) thermal dehydration at 623 K, (d) oxygen oxidation at 623 K, and (e) hydrogen reduction at 623 K.

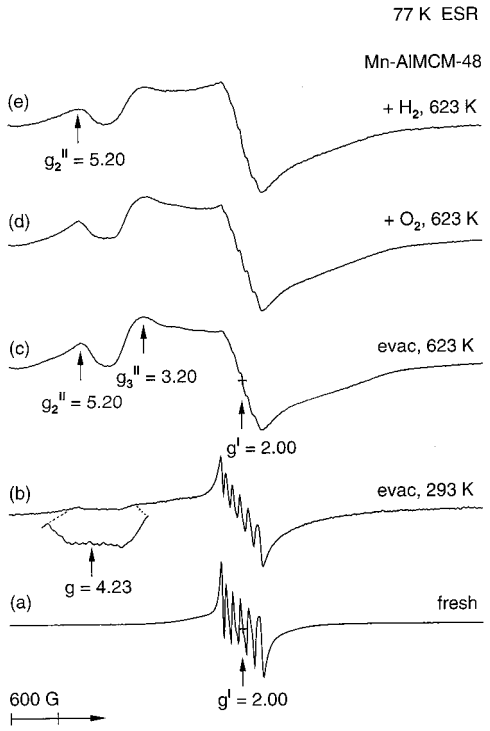

Figure 3. ESR spectra at 77 K of ion-exchanged Mn−AlMCM-48: (a) fresh, (b) evacuation at 293 K, (c) thermal dehydration at 623 K, (d) oxygen oxidation at 623 K, and (e) hydrogen reduction at 623 K. The Si/Al ratio is 50 in the synthesis gel.

in Figure 2e. Oxidation also causes a decrease in the overall ESR intensity, although the relative intensity of species II to III remains the same (Figure 2d). In addition, hyperfine structures are observed for partially dehydrated Mn−MCM-48 at $g = 4.15$ (Figure 2b), which is assigned to Mn(II) species IV and will be discussed in detail later.

The ion-exchanged sample Mn−AlMCM-48-(50) (Si/Mn $\approx$ 1000), which is shown in Figure 3, shows dehydration behavior quite different from that of Mn−MCM-48. For a fresh sample, the sextet of Mn(II) species I with $g = 2.00$ and $A_{iso} = 97$ G is also observed (Figure 3a). However, Mn(II) species I in Mn−AlMCM-48 does not disappear after dehydration at 623 K for 4 h (Figure 3c) or at a temperature as high as 723 K. In addition, subsequent oxidation by oxygen does not produce any new peaks or decrease its overall intensity (Figure 3d,e), and completely dehydrated Mn−AlMCM-48 only shows two peaks around $g = 5.20$ and 3.20, which are attributed to Mn(II) species II (Figure 3c).

As seen in the amplified part in Figure 3b, hyperfine lines are also present around $g = 4.23$ in partially dehydrated Mn−AlMCM-48 and are assigned to Mn(II) species IV. The ESR lines of Mn(II) species IV in partially dehydrated Mn−MCM-48 and Mn−AlMCM-48 are shown in Figure 4. Clearly, one set of sextets centered at $g = 4.15$ with $A = 81.1$ G can be identified in partially dehydrated Mn−MCM-48 (Figure 4a). Under the same treatment, partially dehydrated Mn−AlMCM-48 shows three sextets with g and A values as indicated in Figure 4b. Note that the average A value for Mn(II) species IV in Mn−MCM-48 (Figure 4a) is smaller than that in Mn−AlMCM-48 (Figure 4b). Similar Mn(II) ESR species were also observed by Schreurs in oxide glasses.[21]

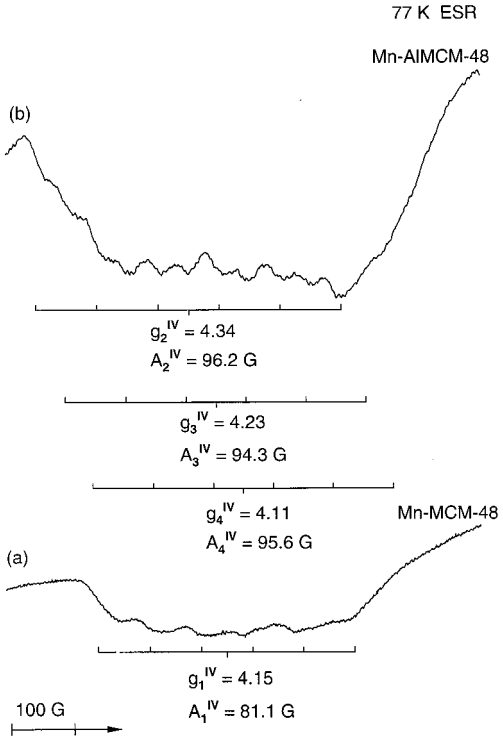

Figure 4. ESR spectra at 77 K of ion-exchanged samples after partial dehydration at 293 K: (a) Mn−MCM-48 and (b) Mn−AlMCM-48.

Synthesized MnMCM-48 materials, where manganese is introduced during synthesis, show dehydration behaviors different from those of Mn(II) ion-exchanged samples. Figure 5 shows the ESR spectra of synthesized MnMCM-48 (Si/Mn = 1000) under the same dehydration treatment. Before treatment, only Mn(II) species I

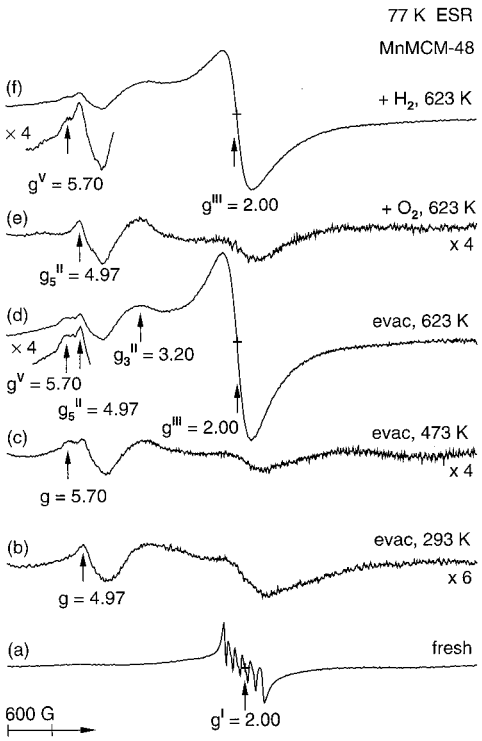

Figure 5. ESR spectra at 77 K of calcined synthesized MnMCM-48: (a) fresh, (b) evacuation at 293 K, (c) thermal dehydration at 623 K, (d) oxygen oxidation at 623 K, and (e) hydrogen reduction at 623 K. The Si/Mn ratio is 1000 in the synthesis gel.

with $g = 2.00$ and $A = 97$ G is observed in calcined and hydrated MnMCM-48 (Figure 5a). After dehydration, Mn(II) species II at $g = 4.97$ and 3.20 and Mn(II) species III at $g = 2.00$ with a line width of 410 G are observed (Figure 5b−d). However, unlike Mn−MCM-48, thermal dehydration of MnMCM-48 at 473 and 623 K produces a new peak at $g = 5.70$ (Figure 5c,d). This new peak disappears upon oxidation (Figure 5e) and is recovered again by hydrogen reduction, but this process is not completely reversible (Figure 5f). This behavior is different from that of Mn(II) species II and therefore is assigned to Mn(II) species V. Upon oxidation, the overall ESR intensity also decreases, and the relative intensity of species II is now much higher than that of Mn(II) species III (Figure 5e). In addition, the broad peak seen at $g = 2.62$ in oxidized Mn−MCM-48 is not observed.

Calcined, synthesized, and hydrated MnAlMCM-48-(50) (Si/Mn ≈ 1000) shows behavior similar to that of Mn−AlMCM-48-(50). The 77 K ESR spectrum of completely dehydrated MnAlMCM-48 is shown in Figure 6a. The sextet hyperfine lines of Mn(II) species I are still visible after 4 h dehydration at 623 K and are probably overlapped by a broad peak from Mn(II) species III. However, after the majority of extraframework Mn(II) ions in MnAlMCM-48 is removed by $CaCl_2$ exchange, Mn(II) species I cannot be observed under the same dehydration condition (Figure 6b). Only a weak broad peak with peak-to-peak line width of 442 G is detected in MnAlMCM-48(Ca), which is Mn(II) species III. This suggests that Mn(II) species III is likely due to framework manganese (II) ions. Note that a weak Mn(II) species III signal is also observed in dehydrated MnAlMCM-48(Ca) due to residual extraframework ions that are not replaced by Ca(II).

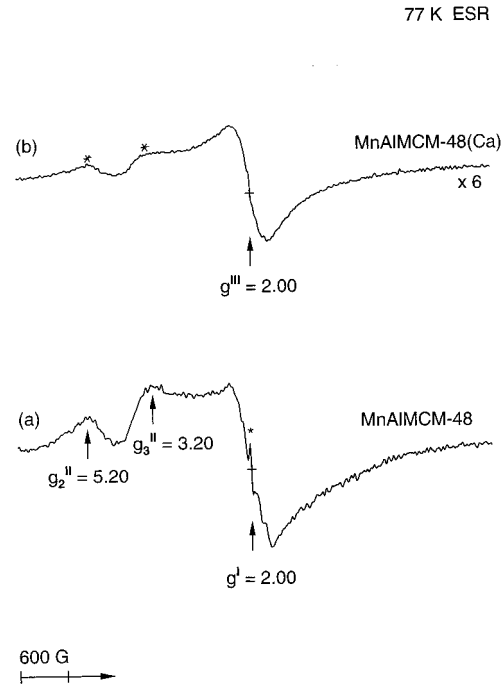

Figure 6. ESR spectra at 77 K obtained after dehydration at 623 K: (a) calcined synthesized MnAlMCM-48 and (b) $CaCl_2$-exchanged MnAlMCM-48(Ca), where a trace of species II marked as (*) exists. The Si/Mn and Si/Al ratios are 1000 and 50, respectively.

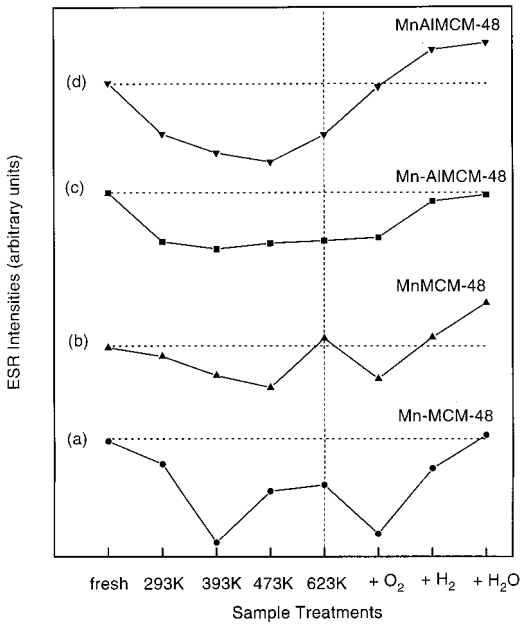

Figure 7. Relative ESR intensities vs various sample treatments: (a) Mn−MCM-48, (b) MnMCM-48, (c) Mn−AlMCM-48, and (d) MnAlMCM-48. The Si/Mn and Si/Al ratios are 1000 and 50, respectively.

The relative overall ESR intensities of ion-exchanged and synthesized Mn-containing MCM-48 samples versus various treatments are shown in Figure 7. The overall ESR intensities of Mn−MCM-48 and MnMCM-48 vary (Figure 7a,b), whereas those of Mn−AlMCM-48 and MnAlMCM-48 change smoothly (Figure 7c,d). Except for MnMCM-48, the other samples show a decrease of the ESR intensity upon dehydration at 623 K (see the vertical dotted line in Figure 7). After further oxidation, the overall ESR intensities of Mn−MCM-48

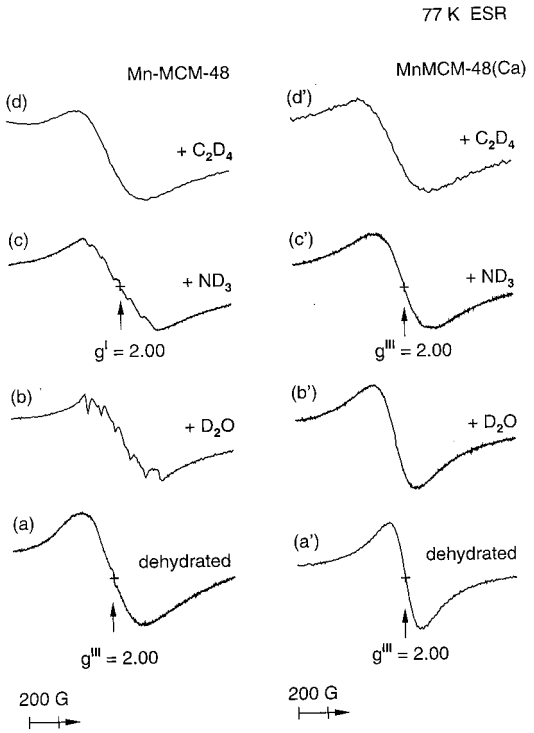

Figure 8. ESR spectra at 77 K of completely dehydrated (a) MnAlMCM-48-(50) and (a′) MnAlMCM-48-(50)(Ca) with 0.1 mol % Mn(II) in the synthesis gel after subsequent adsorption of (b,b′) D_2O for 1 min, (c,c′) ND_3 for 5 min, and (d,d′) C_2D_4 for 3 days.

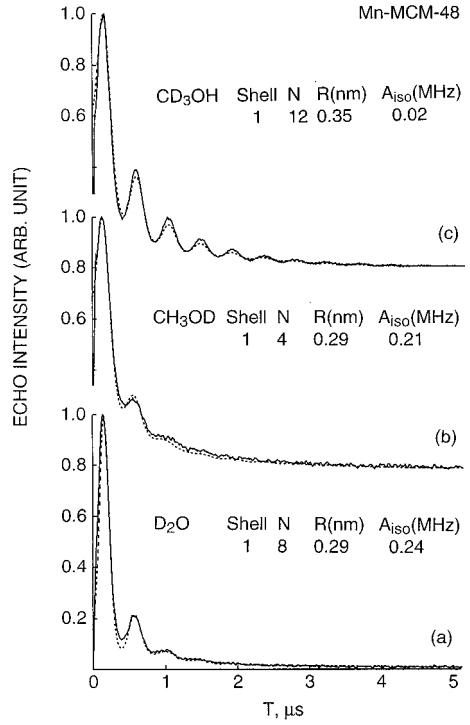

Figure 9. Experimental (—) and simulated (- - -) deuterium three-pulse ESEM at 4 K of Mn(II) ion-exchanged Mn−MCM-48 with adsorbed (a) D_2O, (b) CH_3OD, and (c) CD_3OH (τ = 256 ns).

and MnMCM-48 decrease (Figure 7a,b), but those of Mn−AlMCM-48 and MnAlMCM-48 do not (Figure 7c,d). In addition, after subsequent hydrogen reduction and rehydration, all samples show an increase of the overall ESR intensity. The ESR intensities of Mn−MCM-48 and Mn−AlMCM-48 increase to a level similar to that of fresh samples (Figure 7a,c), but the ESR intensities of synthesized MnMCM-48 and MnAlMCM-48 increase more (Figure 7b,d).

Adsorbate Interactions. After the adsorption of D_2O, methanol, and ND_3 on completely dehydrated Mn−MCM-48 for 14 h, the original octahedral sextet Mn(II) ESR spectra are recovered (same as Figure 2a). However, at early adsorption stages, the adsorption kinetics are different depending on the sample.

The adsorption kinetics of Mn−MCM-48 and Mn-MCM-48(Ca) are compared by their 77 K ESR spectra in Figure 8. As soon as completely dehydrated Mn−MCM-48 (Figure 8a), where only extraframework Mn(II) exists, adsorbs D_2O for 1 min (Figure 8b), the hyperfine sextet of Mn(II) species I is seen clearly. In addition, the sextet is seen after adsorbing ND_3 for 5 min (Figure 8c). However, for completely dehydrated MnMCM-48-(Ca) (Figure 8a′), where most of extraframework Mn(II) ions are removed by $CaCl_2$ exchange, adsorption of D_2O and ND_3 for the same time does not produce Mn(II) species I (Figure 8b′,c′). The adsorption of CH_3OD or CD_3OH on dehydrated samples for 1 min shows spectra similar to parts b and b′ of Figure 8, respectively. So, the Mn(II) ions in MnMCM-48(Ca) are less accessible to adsorbates than those in Mn−MCM-48. In addition, no hyperfine structure is observed after Mn−MCM-48 or MnMCM-48(Ca) adsorbs C_2D_4 for 3 days (Figure 8d,d′). This is probably due to only weak interactions between C_2D_4 and the Mn(II) ions.

ESEM. ESEM measurements of deuterium modulation of Mn(II) ions were performed to identify the probable cation locations in the three types of Mn-containing MCM-48 materials. The three-pulse ESEM spectrum of Mn−MCM-48 with adsorbed D_2O is shown in Figure 9a. The simulation shows one set of eight deuteriums interacting at a distance of 0.29 nm. This indicates that four water molecules are directly coordinated to Mn(II) in Mn−MCM-48. The three-pulse ESEM spectra of Mn−MCM-48 with adsorbed CH_3OD and CD_3OH are shown in parts b and c of Figure 9, respectively. Simulations of the deuterium modulation also indicate that four CH_3OD or CD_3OH molecules directly interact with Mn−MCM-48 in one shell. This is consistent with the simulation for adsorbed D_2O molecules.

Three-pulse ESEM spectra of $CaCl_2$-exchanged Mn-MCM-48(Ca) with adsorbed D_2O, CH_3OD, and CD_3OH are shown in Figure 10. A two-shell model is necessary to simulate the deuterium modulation in this system. For adsorbed D_2O in Figure 10a, the simulation shows two deuteriums and four deuteriums interacting with Mn(II) in two shells at different distances. This indicates that one nearest-neighbor water molecule is directly coordinated to the Mn(II) at a distance of 0.27 nm and two more next-nearest-neighbor water molecules interact at a longer distance of 0.32 nm. The same result is obtained from the simulations of three-pulse ESEM spectra of MnMCM-48(Ca) with adsorbed CH_3OD or CD_3OH (Figure 10b,c). One nearest-neighbor CH_3OD molecule is directly coordinated to Mn(II) at a distance of 0.28 nm and two more next-nearest-neighbor CH_3OD molecules interact at a distance of 0.32 nm.

The ESEM simulation parameters for Mn-containing silicate MCM-48 are summarized in Table 1. It indicates

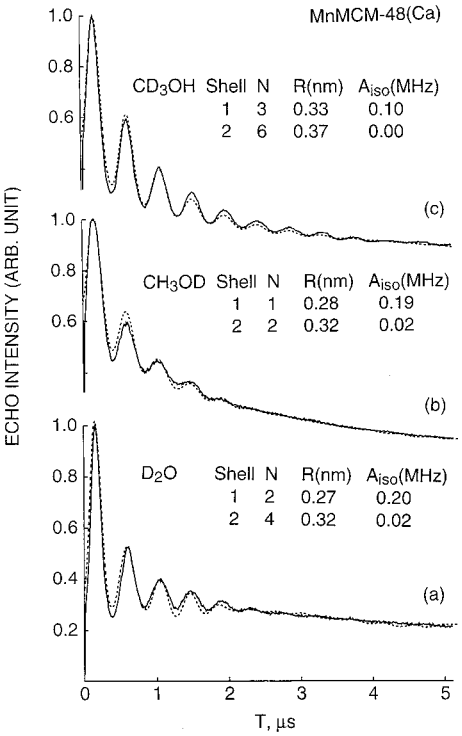

Figure 10. Experimental (—) and simulated (- - -) deuterium three-pulse ESEM at 4 K of synthesized MnMCM-48 with adsorbed (a) D_2O, (b) CH_3OD, and (c) CD_3OH (τ = 256 ns).

Table 1. Simulation Parameters for Three-Pulse ESEM of Mn(II) in Mn-Containing MCM-48 Materials with Adsorbates

samples	adsorbates	shell	N^a	R (nm)^b	A_{iso} (MHz)^c	no. of molecules
Mn−MCM-48	D_2O	1	8	0.29	0.21	4
	CH_3OD	1	4	0.29	0.20	4
	CD_3OH	1	12	0.35	0.02	4
	C_2D_4	1	4	0.37	0.01	1
MnMCM-48	D_2O	1	4	0.28	0.20	2
		2	4	0.34	0.02	2
	CH_3OD	1	2	0.29	0.19	2
		2	2	0.32	0.02	2
	CD_3OH	1	6	0.35	0.01	2
		2	6	0.36	0.00	2
	C_2D_4	1	4	0.45	0.01	1
MnMCM-48(Ca)	D_2O	1	2	0.27	0.21	1
		2	4	0.32	0.02	2
	CH_3OD	1	1	0.28	0.18	1
		2	2	0.31	0.02	2
	CD_3OH	1	3	0.32	0.09	1
		2	6	0.37	0.00	2

[a] Number of ^2D nuclei to the nearest integer. [b] Mn(II)−^2D distance to ±0.01 nm. [c] Isotropic hyperfine coupling of ^2D nuclei to ±10%.

that four water molecules interact with Mn(II) in synthesized MnMCM-48: Two nearest-neighbor water molecules interact at a distance of 0.28 nm, and the other two next-nearest-neighbor water molecules interact at a distance of 0.34 nm. In addition, deuterium modulation simulations also indicate that Mn(II) in Mn−MCM-48 and MnMCM-48 shows similar weak interactions with one C_2D_4 molecule, but no interaction is observed between Mn(II) in MnMCM-48(Ca) and adsorbed C_2D_4. These findings are consistent with the ESR result that Mn(II) in MnMCM-48(Ca) is less accessible to adsorbates than when it is in Mn−MCM-48.

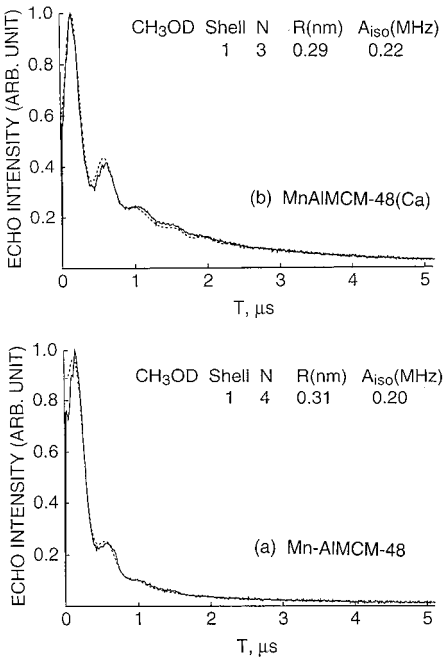

Figure 11. Experimental (—) and simulated (- - -) deuterium three-pulse ESEM at 4 K of (a) Mn(II) ion-exchanged Mn−AlMCM-48-(50) and (b) $CaCl_2$-exchanged MnAlMCM-48-(50)-(Ca) with adsorbed CH_3OD (τ = 256 ns).

Table 2. Simulation Parameters for Three-Pulse ESEM of Mn(II) in Mn-Containing AlMCM-48 Materials with Adsorbates

samples^a	adsorbates	shell	N^b	R (nm)^c	A_{iso} (MHz)^d	no. of molecules
Mn−AlMCM-48	D_2O	1	8	0.29	0.30	4
	CH_3OD	1	4	0.28	0.20	4
	CD_3OH	1	12	0.36	0.01	4
MnAlMCM-48	D_2O	1	4	0.27	0.20	2
		2	4	0.33	0.02	2
	CH_3OD	1	2	0.28	0.20	2
		2	2	0.32	0.02	2
	CD_3OH	1	6	0.35	0.01	2
		2	6	0.36	0.00	2
MnAlMCM-48(Ca)	D_2O	1	2	0.28	0.22	1
		2	4	0.30	0.02	2
	CH_3OD	1	1	0.29	0.21	1
		2	2	0.30	0.02	2
	CD_3OH	1	3	0.34	0.02	1
		2	6	0.35	0.00	2

[a] All Si/Al ratios are 50 ± 3. [b] Number of ^2D nuclei to the nearest integer. [c] Mn((II)−^2D distance to ±0.01 nm. [d] Isotropic hyperfine coupling of ^2D nuclei to ±10%.

For Al-containing MCM-48 samples, similar ESEM simulation results are obtained. Figure 11 shows the three-pulse ESEM spectra of ion-exchanged Mn−AlMCM-48 (Figure 11a) and $CaCl_2$-exchanged synthesized MnMCM-48(Ca) (Figure 11b) with adsorbed CH_3OD. The simulation parameters are given in Table 2. The deuterium simulations indicate that four methanol molecules are coordinated to the Mn(II) in Mn−AlMCM-48 in one shell but one less methanol molecule interacts with the Mn(II) in MnAlMCM-48(Ca). This is consistent with the deuterium modulations in Mn−MCM-48 and MnMCM-48(Ca). Similar to synthesized MnMCM-48, the Mn(II) ions in MnAlMCM-48 also interact with four water molecules in two shells as shown in Table 2.

Discussion

Well-defined cubic MnMCM-48 and MnAlMCM-48-(50) molecular sieves have successfully been synthesized. The ESR signals observed in the Mn-containing MCM-48 materials are attributed to Mn(II) ions.[10−11,18−20] The identical ESR spectra observed for ion-exchanged Mn−MCM-48 (Figure 2a) and for calcined, hydrated MnMCM-48 (Figure 5a) further confirm this assignment for Mn(II) species I because Mn−MCM-48 contains only Mn(II). Other Mn species produced by dehydration are also logically Mn(II) because Mn(II) is relatively stable to the reduction that often accompanies dehydration. However, Mn(III) may also exist in synthesized Mn-MCM-48 materials because its ESR signal is not observable due to its large zero field splitting.[37,38] This is supported by the fact that some extra Mn(II) ions are produced from ESR silent manganese in MnMCM-48 (Figure 7b) or MnAlMCM-48 (Figure 7d). The existence of some Mn(III) has also been suggested in calcined synthesized MnMCM-41.[10,11]

Mn(II) ESR Species. Five Mn(II) species have been observed. Species I can be assigned to octahedral Mn(II) at extraframework sites based on similar ESR parameters obtained in Mn-containing MCM-41[10,11] and in many zeolite materials.[18−20]

Mn(II) peaks similar to those of species II are observed in oxide glasses[39] and manganese complexes,[40] and are usually assigned to zero-field splitting contributions[39,40] with the Mn(II) in a distorted tetrahedral environment, although this symmetry seems speculative. The number of peaks for species II differs among the sample types, suggesting that the zero-field splitting magnitudes also differ. Species II is thus assigned to extraframework Mn(II) with substantial zero-field splitting and possible tetrahedral symmetry.

Species III is a broad singlet obtained in completely dehydrated samples. The coordination is difficult to assign due to its structureless ESR signal. However, species III is more likely to be tetrahedrally coordinated because it is only found in a completely dehydrated system (Figures 2c and 5c) and its total line width is always less than the total line width of octahedral Mn(II). In a similar chemical environment, the Mn(II) hyperfine splitting is greater for six-coordination compared to that of four-coordination.[37,38] Species III is also observed in MnMCM-41 systems, where it was assigned to Mn(II) in a tetrahedral framework site.[11] The same assignment is made here.

Species IV is produced after evacuating Mn−MCM-48 and Mn−AlMCM-48 at 293 K. The peak positions indicate zero field splitting. So, species IV is assigned to distorted octahedral Mn(II) with significant zero field splitting in an extraframework site.

Species V is also a singlet and is produced in Mn-MCM-48 after dehydration. It is also assigned to distorted tetrahedral Mn(II) with significant zero field splitting, but it is different from species II. Species V in MnMCM-48 disappears upon oxidation (Figure 5e), but species II does not, although the overall spectral intensity decreases. Furthermore, species V does not totally recover by reduction treatments (Figure 5f). Therefore, species V behaves differently from extraframework species II and hence is considered to be framework manganese in a tetrahedral site. The various species and their assignments are summarized in Table 3.

Table 3. Observed ESR Species and Their Assignments

sp.	ESR parameter g values (A or ΔH_{pp})[a]	assignments	locations
i	2.00 (97.0 g)	octahed.	extraframework
ii	11.32, 5.20, 4.97, 3.20, 2.62	poss. tetrahed.	extraframework
iii	2.00 (222−433 g)	tetrahed.	framework
iv	4.15 (81.1 g)	tetrahed.?	extraframework
	4.11 (95.6 g)	octahed.	
	4.23 (94.3 g)	octahed.	
	4.34 (96.2 g)	octahed.	
v	5.70	tetrahed.	framework

[a] A is the hyperfine splitting constant, and ΔH_{pp} is the peak-to-peak line width

Manganese Locations. In Mn(II) ion-exchanged samples, Mn−MCM-48 or Mn−AlMCM-48, only extraframework manganese exists. However, in synthesized samples, MnMCM-48 or MnAlMCM-48, both extraframework and framework manganese may exist, as indicated in a previous study on Mn-containing MCM-41 materials.[11] Framework Mn(II) is envisaged as replacing tetrahedrally coordinated Si in the MCM-48 framework.

The dehydration behaviors are different between Mn−MCM-48 and MnMCM-48. In dehydrated Mn−MCM-48 (Figure 3c), species II has four peaks at g = 11.32, 5.20, 3.20, and 2.62. After oxidation, some Mn(II) ions directly coordinate to oxygen to form a broad peak at g = 2.62, some Mn(II) ions are likely oxidized to Mn(III), resulting in a decrease of the overall ESR intensity, and some Mn(II) give species III. In contrast, in dehydrated MnMCM-48, species II contains only two peaks at g = 4.97 and 3.20. After oxidation, the broad peak at g = 2.62 observed in Mn−MCM-48 is not produced, indicating that Mn(II) ions in MnMCM-48 do not directly coordinate to oxygen. In addition, a new species V is observed in dehydrated MnMCM-48. These differences suggest that the manganese locations are different in synthesized and ion-exchanged samples. Therefore, Mn(II) in MnMCM-48 may be in a framework site because in dehydrated, ion-exchanged Mn−MCM-41 only extraframework Mn(II) ions exist.

The adsorbate kinetics are also different between ion-exchanged Mn−MCM-48 and synthesized, Ca(II)-exchanged MnMCM-48(Ca). The Mn(II) ions in dehydrated Mn−MCM-48 quickly react with adsorbates to form octahedral species, as evident from sextet ESR signals. After adsorption of water or methanol, a sextet splitting is observed after 1 min, and after ammonia adsorption, it takes 5 min to observe a sextet splitting. However, the Mn(II) ions in dehydrated MnMCM-48-(Ca), where most extraframework Mn(II) ions are replaced by Ca(II), do not interact with water, methanol, or ammonia to form a sextet splitting within the same time after adsorption. This supports the idea that the Mn(II) ions in MnMCM-48(Ca) exist in framework positions where they are less accessible to adsorbates than they would be in extraframework sites.

(37) Kurshev, V.; Kevan, L.; Parillo, D. J.; Pereira, C.; Kokotailo, G. T.; Gorte, R. J. *J. Phy. Chem.* **1994**, *98*, 10160.
(38) Kijlstra, W. S.; Poels, E. K.; Bliek, A.; Weckhuysen, B. M.; Shoonheydt, R. A. *J. Phys. Chem. B* **1997**, *101*, 309.
(39) Kliava, J. *Phys. Status Solidi B* **1986**, *134*, 411.
(40) Dowsing, R. D.; Gibson, J. F.; Goodgame, D. M. L.; Goodgame, M.; Hayward, P. J. *Nature* **1968**, *219*, 1037.

ESEM simulations also indicate that the number of interacting molecules with Mn(II) ions are different for these two samples (Table 1). After adsorption of water or methanol, Mn(II) in dehydrated Mn−MCM-48 can coordinate four water or methanol molecules in one shell. However, Mn(II) in dehydrated MnMCM-48(Ca) can only coordinate one water or methanol molecule and more weakly interacts with two other molecules. Therefore, there is at least one less adsorbate molecule interacting with possible framework Mn(II). In addition, the ESEM simulations of Mn−AlMCM-48 and MnAlMCM-48(Ca) with various adsorbates also give the same conclusion (Table 2).

TGA measurements also support that manganese is possibly incorporated into the MnMCM-48 framework. In as-synthesized MCM-48, all surfactant molecules are removed completely below 600 K (Figure 1a). However, in as-synthesized MnMCM-48, some surfactant molecules are only removed above 727 K (Figure 1b), which is similar to the case of as-synthesized AlMCM-48 (Figure 1c). A completely condensed silicate framework is nominally neutral, but the incorporation of aluminum or manganese into the framework will create a negatively charged framework.[35,36] This will cause stronger interactions between the surfactants and the framework.

Conclusions

From ESR and ESEM studies on different Mn-containing MCM-48 materials, five Mn(II) species are found and assigned to extraframework and framework positions. Species I at $g = 2.00$ is assigned to extraframework positions with distorted octahedral symmetry. Species II at $g = 11.3$, 5.20, 3.20, and 2.62 is assigned to extraframework Mn(II) ions with zero-field interactions with possible distorted tetrahedral symmetry. Species IV at $g = 4.11-4.34$ is assigned to distorted octahedral extraframework Mn(II) produced upon partial dehydration. Species III and species V are formed during dehydration and are assigned to framework positions with tetrahedral symmetry. The substitution of manganese into the framework is also supported by TGA measurements.

Different properties are observed for extraframework versus framework Mn(II) ions. Framework Mn(II) species V is produced in synthesized MnMCM-48 during dehydration and hydrogen reduction treatment, but it is not observed in ion-exchanged Mn−MCM-48. Framework Mn(II) rehydrates more slowly than does extraframework Mn(II). In addition, framework Mn(II) interacts with fewer adsorbate molecules than does extraframework Mn(II) based on ESEM data.

Acknowledgment. This research was supported by the Robert A. Welch Foundation, the University of Houston Energy Laboratory, and the National Science Foundation.

CM990300J